Journal of Power Sources 198 (2012) 322–328

Contents lists available at SciVerse ScienceDirect

Journal of Power Sources

journal homepage: www.elsevier.com/locate/jpowsour

An approximate solution for solid-phase diffusion in a spherical particle in physics-based Li-ion cell models

Meng Guo, Ralph E. White*

Department of Chemical Engineering, University of South Carolina, Columbia, SC 29208, USA

ARTICLE INFO

Article history:
Received 17 June 2011
Received in revised form 22 August 2011
Accepted 23 August 2011
Available online 30 August 2011

Keywords:
Li ion battery
Modeling
Solid phase diffusion
Eigenfunction

ABSTRACT

An approximate solution is presented for the spherical diffusion equation for the spherical particles in a physics-based lithium-ion battery model. This approximate solution is compared to different numerical and analytic solutions for various boundary conditions. These comparisons reveal that our approximate solution can provide accuracy and time-efficiency in simulation. This approximate solution is much faster than the numerical and truncated analytical solutions at high current rate, and shows better long-time accuracy than the short-time analytical solution. This approximate solution can also be used as the porous electrode model.

1. Introduction

Physics-based models are widely used to predict the behavior of lithium ion cells and batteries [1]. In a typical cell model, each porous electrode is described by a pseudo two-dimensional domain with solid-phase diffusion occurring in spherical particles, for example, at each local position in a porous electrode (see Fig. 1 of Ref. [1]). This solid state diffusion occurs because lithium ions are intercalated or deintercalated through electrochemical reactions at the surface of the solid phase particles [2,3]. For this reason, the concentration of lithium ions at the particle surface is an important variable which is needed in the simulation to determine the reaction rate, for example.

Several numerical methods have been used to solve the solid-phase diffusion equation in the r dimension of spherical particles (the pseudo second dimension) and obtain the surface concentration of lithium ions. For example, the finite difference (FD) [4] and orthogonal collocation on finite elements (OCFE) [5,6] methods have been used. These methods require discretization of the particle radius into node points or elements with interior points; and, consequently, one or more ordinary differential equations (ODEs) are obtained at each point or element (this method is often called the method of lines). However, the computational error caused by the discretization of a continuous domain increases dramatically if there are large concentration gradients at the surface of the particles. If too many node points or elements are applied to reduce the error in discretization, the simulation is severely slowed due to the large number of equations.

The analytic solution to the spherical diffusion equation includes an infinite series. To evaluate this infinite series, the series is approximated by truncating. The truncated series includes a finite number of terms. Evaluation of these terms requires significant computation time for cases with large concentration gradients at the surfaces of the particles, which can occur during pulsing for example.

An approximate analytic solution is presented in this paper to minimize the truncation error associated with implementation of the series with a finite number of terms included in the analytic solution. It is shown that only a few terms are needed in the approximate solution together with an additional term compensating for the truncation error. The resulting approximate solution yields accurate results with less computation time than required for numerical methods or a large number of terms in the analytic solution.

2. Model development

The diffusion of lithium ions in a spherical solid phase particle follows Fick's law and is described by the following partial differential equation (PDE) in the spherical coordinates:

$$\frac{\partial c}{\partial t} = D\frac{1}{r^2}\frac{\partial}{\partial r}\left(r^2\frac{\partial c}{\partial r}\right) \tag{1}$$

$$\text{at} \quad t = 0 \quad \text{for} \quad 0 \le r \le R \quad c(t=0) = c_0 \tag{2}$$

* Corresponding author. Tel.: +1 11 803 777 3270; fax: +1 11 803 777 0973.
E-mail address: white@cec.sc.edu (R.E. White).

0378-7753/$ – see front matter © 2011 Elsevier B.V. All rights reserved.
doi:10.1016/j.jpowsour.2011.08.096

Nomenclature

List of symbols

c	concentration of lithium ions in the solid particles (mol m^{-3})
c_{max}	maximum concentration in particle (mol m^{-3})
C	dimensionless concentration of lithium ions
C_s	dimensionless concentration of lithium ions at particle surface
$\overline{C}$	dimensionless average concentration of lithium ions
D	solid phase diffusion coefficient for lithium ions in the particles (m^2 s^{-1})
e_N	truncation error
$j(t)$	molar flux of lithium at the particle surface (mol m^{-2} s^{-1})
n	index of eigenvalues and eigenfunctions
N	number of eigenfunctions kept in the series
Q_n	eigenfunction
Q_n^{apx}	approximated eigenfunction
r	radial coordinate (m)
R	particle radius (m)
$\bar{r}$	dimensionless radial coordinate
t	time (s)
$\delta(\tau)$	dimensionless molar flux of lithium ions at the particle surface in the $\bar{r}$ direction
λ_n	eigenvalue
τ	dimensionless time

$$\left.\frac{\partial c}{\partial r}\right|_{r=0} = 0 \tag{3}$$

$$-D\left.\frac{\partial c}{\partial r}\right|_{r=R} = j(t) \tag{4}$$

where c is concentration of lithium in the solid particles, D is the solid phase diffusion coefficient for lithium in the particles, $j(t)$ is the time dependent boundary flux, and R is the radius of particle. Assuming that the diffusivity D and the particle radius R are constants, these model equations can be rewritten in the dimensionless form by choosing the following dimensionless variables:

$$C = \frac{c}{c_{max}} \tag{5}$$

$$\tau = \frac{Dt}{R^2} \tag{6}$$

$$\delta(\tau) = \frac{j(t)R}{D(t)c_{max}} \tag{7}$$

$$\bar{r} = \frac{r}{R} \tag{8}$$

where c_{max} is the maximum lithium concentration in the particle. The dimensional equations (1) through (4) can be converted into the following dimensionless equations by using Eqs. (5)–(8)

$$\frac{\partial C}{\partial \tau} = \frac{1}{\bar{r}^2}\frac{\partial}{\partial \bar{r}}\left(\bar{r}^2\frac{\partial C}{\partial \bar{r}}\right) \tag{9}$$

$$C(\tau = 0) = C_0 \tag{10}$$

$$\left.\frac{\partial C}{\partial \bar{r}}\right|_{\bar{r}=0} = 0 \tag{11}$$

$$\left.\frac{\partial C}{\partial \bar{r}}\right|_{\bar{r}=1} = -\delta(\tau) \tag{12}$$

The analytic solution to these equations is [7]

$$C(\bar{r},\tau) = C_0 + \frac{3}{10}\delta(\tau) - \frac{\delta(\tau)}{2}\bar{r}^2 - 3\int_0^\tau \delta(\tau')\,d\tau' + 2\sum_{n=1}^{\infty}\frac{\sin(\lambda_n\bar{r})}{\bar{r}\lambda_n^2\sin(\lambda_n)}\delta(\tau) - 2\sum_{n=1}^{\infty}\frac{\sin(\lambda_n\bar{r})}{\bar{r}\sin(\lambda_n)}e^{-\lambda_n^2\tau}\int_0^\tau \delta(\tau')e^{\lambda_n^2\tau'}d\tau' \tag{13}$$

The last two terms in Eq. (13) can be combined by letting

$$Q_n(\tau) = -2\,e^{-\lambda_n^2\tau}\int_0^\tau \delta(\tau')e^{\lambda_n^2\tau'}d\tau' \tag{14}$$

Eq. (13) then becomes

$$C(\bar{r},\tau) = C_0 + \frac{3}{10}\delta(\tau) - \frac{\delta(\tau)}{2}\bar{r}^2 - 3\int_0^\tau \delta(\tau')\,d\tau' + \sum_{n=1}^{\infty}\frac{\sin(\lambda_n\bar{r})}{\bar{r}\sin(\lambda_n)}\left[Q_n(\tau) + \frac{2\delta(\tau)}{\lambda_n^2}\right] \tag{15}$$

Eq. (14) can be written as a differential equation by taking the derivative of each side of Eq. (14) with respect to τ:

$$\frac{dQ_n}{d\tau} = -\lambda_n^2 Q_n(\tau) - 2\delta(\tau) \quad \text{for} \quad n = 1 \quad \text{to} \quad \infty \tag{16}$$

with

$$Q_n(\tau = 0) = 0 \quad \text{for } n = 1 \text{ to } \infty \tag{17}$$

where λ_n is the nth eigenvalue calculated from the following equation

$$\lambda_n - \tan\lambda_n = 0 \quad n = 1, 2, \cdots \tag{18}$$

Note that when $\delta(\tau)$ is a constant, Eq. (16) yields

$$Q_n(\tau) = -\frac{2\delta}{\lambda_n^2}[1 - \exp(-\lambda_n^2\tau)] \tag{19}$$

at the surface of the particle

$$C_s(\tau) = C(\bar{r} = 1,\ \tau) \tag{20}$$

Eq. (15) can be used to write the dimensionless surface concentration, $C_s(\tau)$, in terms of the average concentration and the eigenfunction, Q_n:

$$C_s(\tau) = \overline{C}(\tau) + \sum_{n=1}^{\infty} Q_n(\tau) \tag{21}$$

where $\overline{C}(\tau) = 3\int_0^1 \bar{r}^2 C(\bar{r},\tau)\,d\bar{r}$ is the average concentration and is determined by

$$\frac{d\overline{C}}{d\tau} = -3\delta(\tau) \quad \bar{C}(\tau = 0) = C_0 \tag{22}$$

Eq. (21) presents the theoretical form for the complete solution for $C_s(\tau)$ if an infinite number of terms are included in the series. However, to calculate a value for the surface concentration, one normally retains N terms in the series by using a truncated solution:

$$C_s^{trun}(\tau) = \overline{C}(\tau) + \sum_{n=1}^{N} Q_n(\tau) + e_N(\tau) \tag{23}$$

where the truncation error, $e_N(\tau)$, between the truncated solution given in Eq. (23) and the complete solution given in Eq. (21) is given by

$$e_N(\tau) = \sum_{n=N+1}^{\infty} Q_n(\tau) \tag{24}$$

Now, let's develop an approximation for this truncation error. To do so, let's find an approximate eigenfunction Q_n^{apx}. That is, let

$$Q_n^{apx} = -\frac{2\delta(\tau)}{\lambda_n^2}[1 - \exp(-\lambda_n^2\tau)] \tag{25}$$

(note that this is the eigenfunction for a constant δ given in Eq. (19)). Next, take the derivative of both sides of Eq. (25) with respect to τ to obtain the following equation

$$\frac{dQ_n^{apx}}{d\tau} = -\lambda_n^2 Q_n^{apx} - 2\delta(\tau) - \frac{2}{\lambda_n^2}\frac{d\delta(\tau)}{d\tau}[1 - \exp(-\lambda_n^2\tau)] \quad \text{with} \quad Q_n^{apx}\big|_{\tau=0} = 0 \tag{26}$$

For large values of n, the nth eigenvalue λ_n will be large enough to satisfy the relationship

$$2\delta(\tau) \gg \frac{2}{\lambda_n^2}\frac{d\delta(\tau)}{d\tau}[1 - \exp(-\lambda_n^2\tau)] \tag{27}$$

and Eq. (26) can be simplified to

$$\frac{dQ_n^{apx}}{d\tau} \approx -\lambda_n^2 Q_n^{apx} - 2\delta(\tau) \tag{28}$$

Next, let the approximate truncation error be

$$e_N^{apx}(\tau) = \sum_{n=N+1}^{\infty} Q_n^{apx}(\tau) \tag{29}$$

where N is large enough to insure that Eq. (27) is valid. Since Q_n^{apx} is a function of n, the summation $\sum_{n=N+1}^{\infty} Q_n^{apx}$ can be converted approximately to the integration of Q_n^{apx} with n:

$$\sum_{n=N+1}^{\infty} Q_n^{apx} = \int_{N+1}^{\infty} Q_n^{apx}\, dn \tag{30}$$

For large n, it is known that

$$\lambda_n \approx \left(\frac{1}{2} + n\right)\pi \tag{31}$$

Consequently,

$$d\lambda_n \cong \pi\, dn \tag{32}$$

Substitution of Eqs. (25) and (32) into Eq. (30) yields

$$\sum_{n=N+1}^{\infty} Q_n^{apx} = -\frac{1}{\pi}\int_{\lambda_{N+1}}^{\infty} \frac{2\delta(\tau)}{\lambda_n^2}[1 - \exp(-\lambda_n^2\tau)]\, d\lambda_n \tag{33}$$

The right hand side of Eq. (33) can be integrated analytically to obtain:

$$-\frac{1}{\pi}\int_{\lambda_{N+1}}^{\infty} \frac{2\delta(\tau)}{\lambda_n^2}[1 - \exp(-\lambda_n^2\tau)]\, d\lambda_n = -2\delta(\tau)\left[\frac{1 - \exp(-\lambda_{N+1}^2\tau)}{\pi\lambda_{N+1}} + \sqrt{\frac{\tau}{\pi}}\,\mathrm{erfc}(\lambda_{N+1}\sqrt{\tau})\right] \tag{34}$$

Since

$$\frac{1}{\pi\lambda_{N+1}} = \frac{1}{\pi}\int_{\lambda_{N+1}}^{\infty}\frac{1}{\lambda_n^2}\, d\lambda_n \approx \sum_{n=N+1}^{\infty}\frac{1}{\lambda_n^2} \tag{35}$$

substitute Eq. (35) into (34) and to obtain

$$-\frac{1}{\pi}\int_{\lambda_{N+1}}^{\infty} \frac{2\delta(\tau)}{\lambda_n^2}[1 - \exp(-\lambda_n^2\tau)]\, d\lambda_n = -2\delta(\tau)\left\{\left(\sum_{n=N+1}^{\infty}\frac{1}{\lambda_n^2}\right)[1 - \exp(-\lambda_{N+1}^2\tau)] + \sqrt{\frac{\tau}{\pi}}\,\mathrm{erfc}(\lambda_{N+1}\sqrt{\tau})\right\} \tag{36}$$

The derivation from Eqs. (34) to (36) effectively removes the error generated from converting addition to integration (Eq. (30)) because Eq. (36) satisfies the long-time accuracy. That is, as $\tau\to\infty$, $\exp(-\lambda_n^2\tau)\to 0$, and according to Eq. (25),

$$Q_n^{apx} = -\frac{2\delta(\tau)}{\lambda_n^2} \quad as\ \tau\to\infty \tag{37}$$

therefore

$$\sum_{n=N+1}^{\infty} Q_n^{apx} = -2\delta(\tau)\sum_{n=N+1}^{\infty}\frac{1}{\lambda_n^2} \quad as\ \tau\to\infty \tag{38}$$

Also as $\tau\to\infty$, $\sqrt{(\tau/\pi)}\,\mathrm{erfc}(\lambda_{N+1}\sqrt{\tau})\to 0$, and the right-hand-side of Eq. (36) becomes

$$-2\delta(\tau)\left\{\left(\sum_{n=N+1}^{\infty}\frac{1}{\lambda_n^2}\right)[1 - \exp(-\lambda_{N+1}^2\tau)] + \sqrt{\frac{\tau}{\pi}}\,\mathrm{erfc}(\lambda_{N+1}\sqrt{\tau})\right\} = -2\delta(\tau)\sum_{n=N+1}^{\infty}\frac{1}{\lambda_n^2} \tag{39}$$

Comparing Eq. (38) and (39), we obtain that the following approximation

$$\sum_{n=N+1}^{\infty} Q_n^{apx} \approx -2\delta(\tau)\left\{\left(\sum_{n=N+1}^{\infty}\frac{1}{\lambda_n^2}\right)[1 - \exp(-\lambda_{N+1}^2\tau)] + \sqrt{\frac{\tau}{\pi}}\,\mathrm{erfc}(\lambda_{N+1}\sqrt{\tau})\right\} \quad as\ \ \tau\to\infty \tag{40}$$

which has good accuracy for $\tau\to\infty$.

Since

$$\sum_{n=1}^{\infty}\frac{1}{\lambda_n^2} = \frac{1}{10} \tag{41}$$

we can write

$$\sum_{n=N+1}^{\infty}\frac{1}{\lambda_n^2} = \sum_{n=1}^{\infty}\frac{1}{\lambda_n^2} - \sum_{n=1}^{N}\frac{1}{\lambda_n^2} = \frac{1}{10} - \sum_{n=1}^{N}\frac{1}{\lambda_n^2} \tag{42}$$

Substitution of Eq. (42) into (40) yields

$$\sum_{n=N+1}^{\infty} Q_n^{apx} \approx -2\delta(\tau)\left\{\left(\frac{1}{10} - \sum_{n=1}^{N}\frac{1}{\lambda_n^2}\right)[1 - \exp(-\lambda_{N+1}^2\tau)] + \sqrt{\frac{\tau}{\pi}}\,\mathrm{erfc}(\lambda_{N+1}\sqrt{\tau})\right\} \tag{43}$$

Thus, the approximate truncation error becomes

$$e_N^{apx}(\tau) = -2\delta(\tau)\left\{\left(\frac{1}{10} - \sum_{n=1}^{N}\frac{1}{\lambda_n^2}\right)[1 - \exp(-\lambda_{N+1}^2\tau)] + \sqrt{\frac{\tau}{\pi}}\,\mathrm{erfc}(\lambda_{N+1}\sqrt{\tau})\right\} \tag{44}$$

Using Eq. (44) to approximate the truncation error in Eq. (23), we obtain our approximate solution for the surface concentration:

$$C_s^{\mathrm{apx}}(\tau) = \overline{C}(\tau) + \sum_{n=1}^{N} Q_n(\tau) - 2\delta(\tau)\left\{\left(\frac{1}{10} - \sum_{n=1}^{N}\frac{1}{\lambda_n^2}\right)[1 - \exp(-\lambda_{N+1}^2\tau)] + \sqrt{\frac{\tau}{\pi}}\,\mathrm{erfc}(\lambda_{N+1}\sqrt{\tau})\right\} \quad (45)$$

when $\delta(\tau)$ is a constant, Eq. (45) becomes

$$C_s^{\mathrm{apx}}(\tau) = C_0 - 3\delta\tau - 2\delta\left\{\left(\frac{1}{10} - \sum_{n=1}^{N}\frac{1}{\lambda_n^2}\right)[1 - \exp(-\lambda_{N+1}^2\tau)] + \sqrt{\frac{\tau}{\pi}}\,\mathrm{erfc}(\lambda_{N+1}\sqrt{\tau})\right\} - \sum_{n=1}^{N}\frac{2\delta}{\lambda_n^2}[1 - \exp(-\lambda_n^2\tau)] \quad (46)$$

when $\delta(\tau) = -\sin(\tau)$ Eq. (45) becomes

$$C_s^{\mathrm{apx}}(\tau) = C_0 - 3[\cos(\tau) - 1] + 2\sin(\tau)\left\{\left(\frac{1}{10} - \sum_{n=1}^{N}\frac{1}{\lambda_n^2}\right)[1 - \exp(-\lambda_{N+1}^2\tau)] + \sqrt{\frac{\tau}{\pi}}\,\mathrm{erfc}(\lambda_{N+1}\sqrt{\tau})\right\} + \sum_{n=1}^{N}\left[\frac{2e^{-\lambda_n^2\tau} - 2\cos(\tau) + 2\lambda_n^2\sin(\tau)}{\lambda_n^4 + 1}\right] \quad (47)$$

Eq. (45) is our approximate solution for the dimensionless surface concentration as a function of time. It will be shown below that our approximate solution provides an accurate value for the surface concentration with only a few terms ($N = 5$, *e.g.*) in the series in Eq. (45) in comparison to the truncated solution (Eq. (23)) with a large number of terms. It is also shown that our approximate solution with only a few terms agrees well with numerical solutions for both constant boundary flux and time-dependent boundary flux expressions.

3. Results and discussion

Our approximate solution for the surface concentration, $C_s^{\mathrm{apx}}(\tau)$, can be obtained in analytic form when δ is a constant or a simple function of dimensionless time or by numerically solving $N + 1$ ODEs (one for $\overline{C}$ and N for Q_1 through Q_N). The simulations presented below were based on the discharge of the positive electrode in a lithium ion pouch cell (the design parameters for this type of cell are available in Ref. [8] and listed in Table 1). Where the dimensionless flux equivalent to 1 C rate is calculates as

$$\delta_{1C} = \frac{I_{1C}R_p}{\mathrm{DFS}_p c_{\max}} = 0.200452 \quad (48)$$

The initial condition is $C_0 = 0.5$ and the simulation stops when C_s reaches 0.95.

3.1. Comparisons with truncated solutions

Comparisons between our approximate solution and the truncated solutions are presented in Fig. 1. In this case, the boundary flux $\delta = -20$ is equivalent to 100 C rate. As shown in Fig. 1, with only 5 terms, our approximate solution provides the same accuracy as the truncated solution with 5000 terms. Note that the 300 term truncated solution is not accurate.

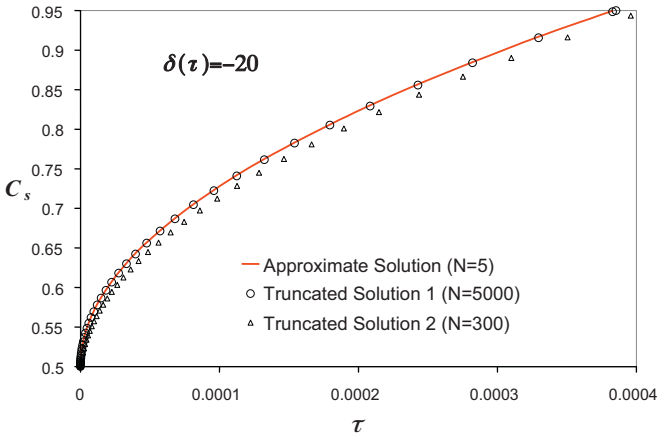

Fig. 1. The comparison between the reformulated eigenfunction solution and truncated solutions.

3.2. Comparisons with numerical solutions

To compare our approximate solution to numerical solutions, two commonly used numerical approaches were used: the finite difference (FD) method and the orthogonal collocation on finite element (OCFE) method. As shown in Fig. 2(a), the five-term approximate solution agrees well with FD solution 1 with 2000 node points. If the number of node points is reduced to 100, the FD solution 2 shows poor accuracy. The FD solution 1 deviates slightly from the reformulated eigenfunction solution around the initial

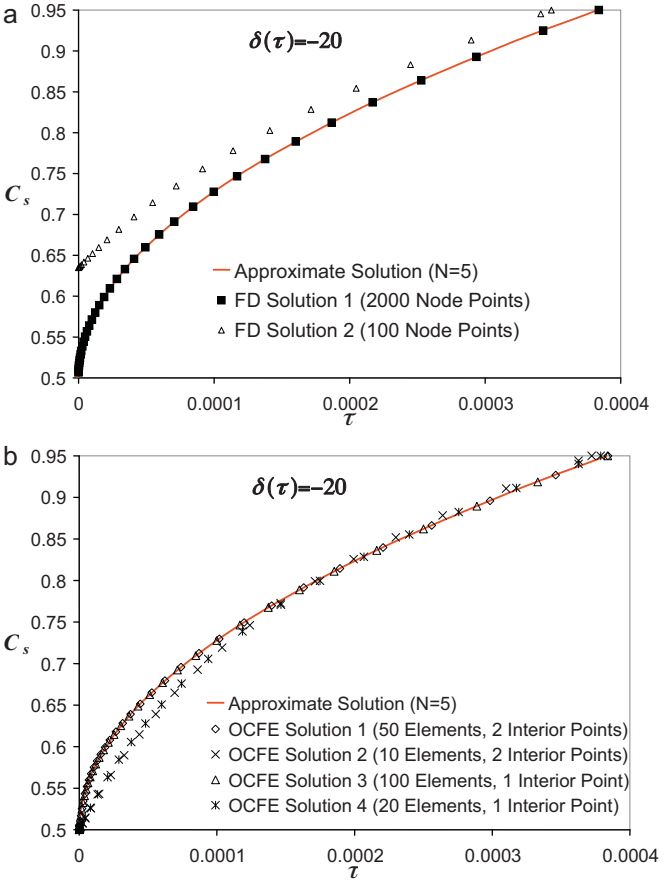

Fig. 2. The comparison between the reformulated eigenfunction solution and (a) FD solutions, (b) OCFE solutions.

Table 1
The design parameters for positive electrode of MSA pouch cell.

Symbol	Description	Value	Unit
I_{1C}	1 C rate current	1.656	A
D^a	Diffusion coefficient in the particle	1.213×10^{-14}	$m^2\ s^{-1}$
S_p	Total electroactive surface area of positive electrode	1.167	m^2
c_{max}	Maximum concentration in particle	51,410	$mol\ m^{-3}$
F	Faraday's constant	96,487	$C\ mol^{-1}$
R_p	radius of particle	8.5×10^{-6}	m

[a] Evaluated at 30 °C using Arrhenius's correlation with activation energy of 29 kJ mol^{-1}.

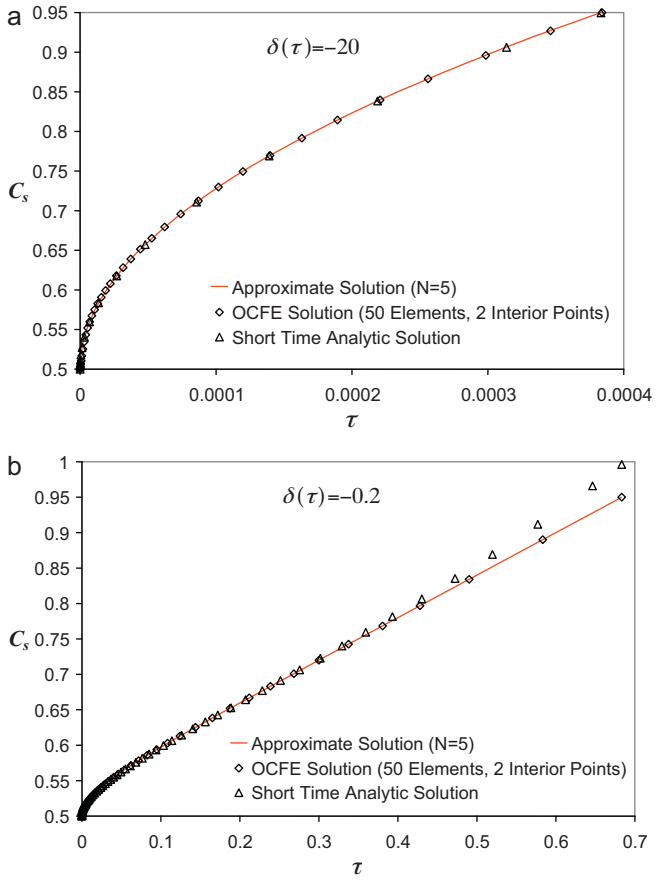

Fig. 3. The surface concentration with periodic boundary flux (a) low frequency, (b) high frequency.

time $\tau = 0$, even though these two solutions agree perfectly with each other over the most of the time range. In FD solution 1, the calculated initial value is $C_s = 0.5067$ at $\tau = 0$, which is not consistent with the set value 0.5. The reason is that, in the FD method, the dependent variables at the two boundary points are determined by algebraic equations, and the error is caused in the initialization of DAE system. For our approximate solution, all dependent variables are determined by ODEs and no initialization is needed, so the solution can start exactly at the set value.

Fig. 2(b) presents a comparison between our approximate solution and the OCFE solutions with different settings. As shown in the figure, the five-term approximate solution agrees with the OCFE solutions 1 and 3 in which finer element mesh size is applied and more equations are included to ensure sufficient accuracy. The OCFE solutions 2 and 4 with larger element mesh size and less equations have significant error. In OCFE method, all equations are ODEs and no initialization is involved, so consistent initial conditions can be obtained.

The solution times for different approaches are listed in Table 2. The reformulated eigenfunction solution is much faster than the other numerical solutions with the same level of accuracy. Being time-efficient is a great advantage for the reformulated solution over the numerical solutions. It's also found in Table 2, the OCFE method is faster than the FD method, and furthermore, there is no initial error for OCFE method; therefore in the following case studies, the OCFE solution with 50 elements and 2 interior points is used to validate the accuracy of our approximate solution.

Table 2
The simulation time for different approaches.

Approach	Solution time (s)
Approximate solution ($N = 5$) (Eq. (45))	0.015
FD solution 1 (2000 points)	4.98
OCFE solution 1 (50 elements and interior points)	0.391
OCFE solution 3 (100 elements and interior point)	0.406

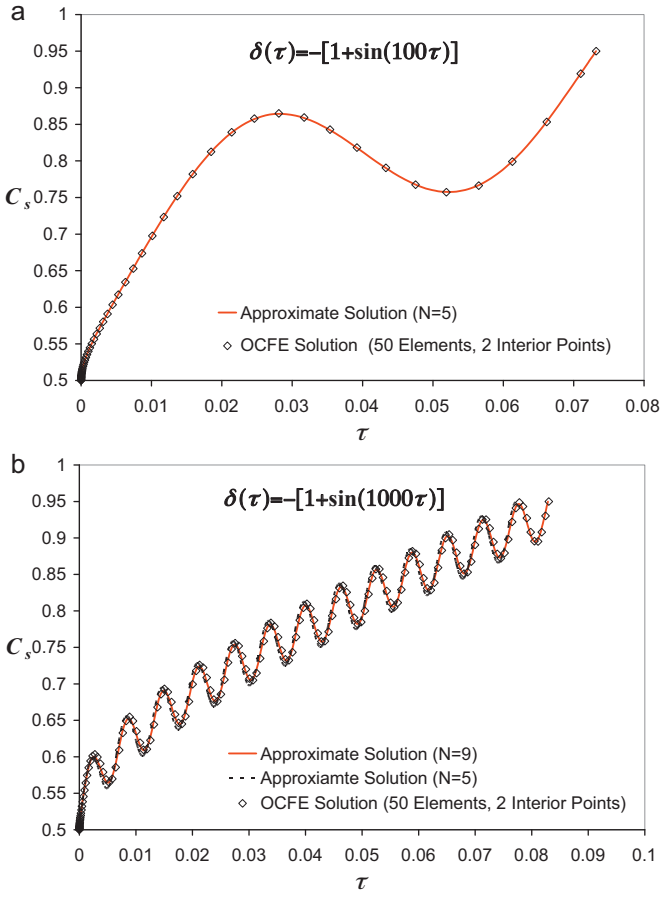

Fig. 4. The comparison between the reformulated eigenfunction solution and short-time analytic solution (a) large boundary flux, (b) small boundary flux.

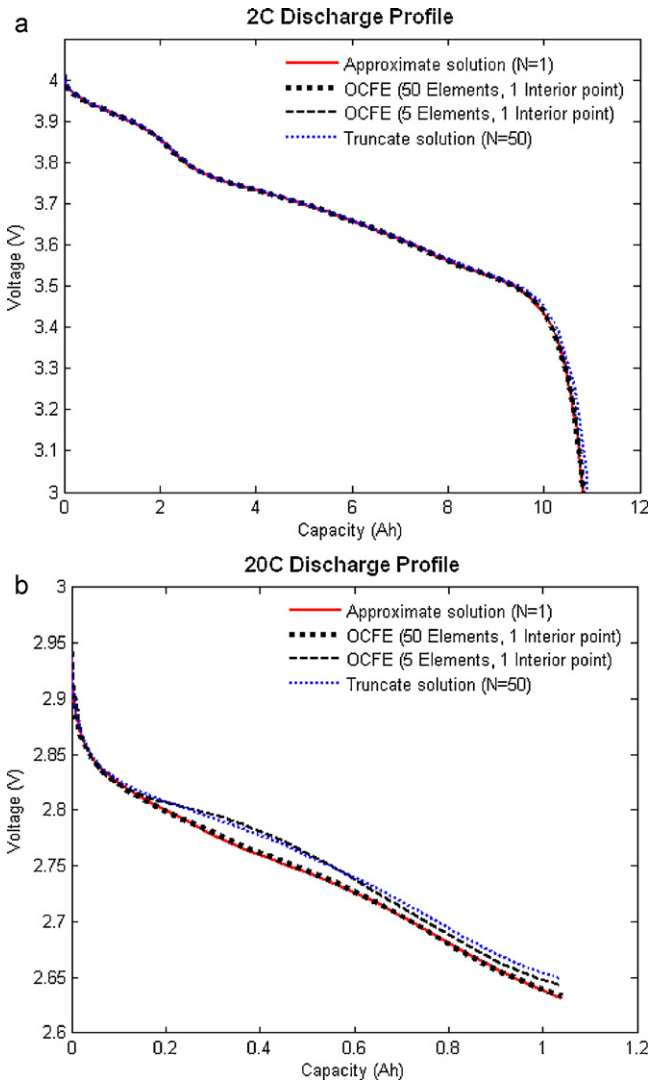

Fig. 5. The simulated (a) 2 C and (b) 20 C discharge profiles using pseudo-2D model.

3.3. Comparisons with the short-time analytic solutions

Using the method described by Atlung, et al. [9] if the boundary flux δ is constant, a short-time analytic solution for C_s can be obtained (see Appendix A) as follows:

$$C_s(\tau) = C_0 - \delta[1 - e^{\tau}\,\mathrm{erfc}(-\sqrt{\tau})] \tag{49}$$

Fig. 3(a) shows a comparison between our approximate solution and the short-time solution with a large boundary flux $\delta = -20$. According to this figure, the predictions from our approximate solution, the short-time analytic solution, and the OCFE solution are consistent. Fig. 3(b) presents the comparison with small boundary flux $\delta = -0.2$, which corresponds to a 1 C discharge rate. In this case, since it takes longer time for C_s to charge from 0.5 to 0.95, the short-time analytic solution loses its accuracy and deviates from the other two curves at the final stage, but our approximate solution still agrees well with the OCFE solution (which can be safely considered as accurate) over the entire time range.

The above comparisons show that the use short-time analytic solution is only valid over a small time range. Another limitation for the short-time analytic solution is that it only works for a constant boundary flux. Therefore, our approximate solution is more useful.

3.4. With time-dependent boundary flux

In this paper, two time-dependent boundary flux conditions are considered: $\delta(\tau) = -[1 + \sin(100\tau)]$ and $\delta(\tau) = -[1 + \sin(1000\tau)]$. The results are presented in Fig. 4(a) and (b). In Fig. 4(a), at a lower frequency, the five-term eigenfunction solution shows good accuracy as validated by the OCFE solution. In Fig. 3(b), however, the five-term eigenfunction solution becomes less accurate when the frequency is increased to 1000, and nine eigenfunction terms are needed for this case ($N = 9$). The reason for the additional terms can be explained by considering Eq. (27). Since the time-derivative of the boundary flux ($d\delta/d\tau$) increases with frequency, a larger λ_n is required to keep the right hand side of Eq. (27) small enough; and, therefore, more eigenfunctions are needed in the series.

3.5. Application in porous electrode model

Our approximate solution can also be used to simply the porous electrode model (the Pseudo-2D model) [1,2]. The 2 C and 20 C discharge profiles simulated by pseudo-2D model with different solution approaches for the solid-phase diffusion equations are presented in Fig. 5(a) and (b), and in each plot, the OCFE solution with 50 elements and 1 interior point is used as the complete solution. As shown in Fig. 5(a), at the 2 C rate, both the 1-term approximate solution and the 5-element OCFE solution agree with the complete solution but the 50-term truncate solution loses accuracy at the end of discharge. As shown in Fig. 5(b), when the discharge rate increases to 20 C, the 1-term approximate solution still shows good accuracy but the 5-element OCFE solution and the 50-term truncate solution deviate significantly from the complete solution.

4. Conclusion

An approximate solution is presented for the surface concentration in a spherical particle with a constant or a time-dependent flux boundary condition at the surface. Our approximate solution for the surface concentration (Eq. (45)) applies for various boundary conditions: large constant flux for short time, small constant flux for long time, low frequency periodic boundary flux, and high frequency periodic boundary flux. This approximate solution has proven to be advantageous over the commonly used solutions:

1) It contains much fewer terms than the truncate solution as the truncation error is effectively approximated.
2) It shows the same level of accuracy with numerical solutions including large numbers of node points or mesh elements, but is much faster.
3) It shows much better long-time accuracy than the short-time analytical solution.
4) This approximate solution also works for the porous-electrode model in which the particle surface flux is dynamic.

Therefore, this approximate solution method greatly improves the simulation efficiency and accuracy of physics-based Li-ion cell models.

Appendix A. The short-time solution for particle diffusion

Dimensionless governing equation for solid-phase diffusion:

$$\frac{\partial C}{\partial \tau} = \frac{1}{\bar{r}^2}\frac{\partial}{\partial \bar{r}}\left(\bar{r}^2\frac{\partial C}{\partial \bar{r}}\right) \tag{A-1}$$

Initial condition:

$$C(\tau = 0) = C_0 \tag{A-2}$$

Boundary conditions:

$$\left.\frac{\partial C}{\partial \bar{r}}\right|_{\bar{r}=0} = 0 \tag{A-3}$$

$$-\left.\frac{\partial C}{\partial \bar{r}}\right|_{\bar{r}=1} = \delta \tag{A-4}$$

Taking Laplace-transformation $C(\tau, \bar{r}) \rightarrow u(s, \bar{r})$ for governing equation

$$su - C_0 = \frac{1}{\bar{r}^2}\frac{\partial}{\partial \bar{r}}\left(\bar{r}^2 \frac{\partial u}{\partial \bar{r}}\right) \tag{A-5}$$

Solving Eq. (A-5) to obtain

$$u = C_2 \frac{\sinh(\sqrt{s}\bar{r})}{\bar{r}} + C_1 \frac{\cosh(\sqrt{s}\bar{r})}{\bar{r}} + \frac{C_0}{s} \tag{A-6}$$

where C_1 and C_2 are integral constants to be determined by boundary conditions.

As u cannot be infinitely large at $\bar{r} = 0$, according to Eq. (A-6)

$$C_1 = 0 \tag{A-7}$$

and

$$u = C_2 \frac{\sinh(\sqrt{s}\bar{r})}{\bar{r}} + \frac{C_0}{s} \tag{A-8}$$

Applying boundary condition at $x = 1$

$$\left.\frac{\partial C}{\partial \bar{r}}\right|_{\bar{r}=1} = -C_2 \sinh(\sqrt{s}) + C_2\sqrt{s}\cosh(\sqrt{s})$$
$$= -\frac{\delta}{s} \Rightarrow C_2 = \frac{\delta}{s\left[\sinh(\sqrt{s}) - \sqrt{s}\cosh(\sqrt{s})\right]} \tag{A-9}$$

and

$$u = \frac{\sinh(\sqrt{s}\bar{r})\delta}{\bar{r}s\left[\sinh(\sqrt{s}) - \sqrt{s}\cosh(\sqrt{s})\right]} + \frac{C_0}{s} \tag{A-10}$$

According to Eq. (A-10), the surface concentration at $\bar{r} = 1$ can be rewritten as

$$u_s = \frac{\delta}{s\sqrt{s}\coth(\sqrt{s}) - s} + \frac{C_0}{s} \tag{A-11}$$

As $s \rightarrow \infty$, $\coth(\sqrt{s}) \rightarrow 1$, and

$$u_s = \frac{\delta}{s\sqrt{s} - s} + \frac{C_0}{s} \tag{A-12}$$

Take inverse Laplace transformation $u_s(s) \rightarrow C_s(\tau)$ for Eq. (A-12) and obtain

$$C_s = C_0 - \delta[1 - e^{\tau}\mathrm{erfc}(-\sqrt{\tau})] \tag{A-13}$$

References

[1] S. Santhanagopalan, Q. Guo, P. Ramadass, R.E. White, J. Electrochem. Soc. 156 (2) (2006) 620.
[2] T.F. Fuller, M. Doyle, J. Newman, J. Electrochem. Soc. 141 (1) (1994) 1–10.
[3] M. Doyle, J. Newman, J. Power Sources 54 (1995) 46–51.
[4] H. Levy, F. Lessman, Finite Difference Equations, Dover publications, Dover, 1992.
[5] G.F. Carey, B.A. Finlayson, Chem. Eng. Sci. 30 (1975) 587–596.
[6] S. Arora, S.S. Dhaliwal, V.K. Kukreja, Appl. Math. Comput. 171 (2005) 358–370.
[7] S. Liu, Solid State Ionics 177 (53) (2006).
[8] M. Guo, G. Sikha, R.E. White, J. Electrochem. Soc. 158 (2) (2011) A122–A132.
[9] S. Atlung, K. West, T. Jacobsen, J. Electrochem. Soc. 126 (8) (1979) 1311–1321.